Asian Journal of Chemistry; Vol. 36, No. 8 (2024), 1865-1871

ASIAN JOURNAL OF CHEMISTRY

https://doi.org/10.14233/ajchem.2024.31953

Synthesis, X-Ray Crystal Structure, Solid State Electrical and Optical Properties of New Copper(II) Complex with 1,10-Phenanthroline Ligand[†]

Saikat Sarkar[1,*], Avijit Sarkar[2], Yildirim Aydogdu[3], Fethi Dagdelen[4], Sougata Sarkar[5] and Krishna Chattopadhyay[6]

[1]Department of Chemistry, Chakdaha College, Chakdaha-741222, India
[2]Department of Chemistry, Bhairab Ganguly College, Kolkata-700056, India
[3]Department of Physics, Gazi University, Ankara, Turkey
[4]Department of Physics, Firat University, Elazig, Turkey
[5]Department of Chemistry, Ramakrishna Mission Vivekananda Centenary College, Rahara-700118, India
[6]School of Chemical Sciences, Indian Association for the Cultivation of Science, Kolkata-700032, India
[†]Dedicated to Late Prof. Kamalendu Dey, Ex-Emeritus Professor, University of Kalyani, Kalyani, India

*Corresponding author: E-mail: saikat_s@rediffmail.com

Received: 15 May 2024; *Accepted*: 15 June 2024; *Published online*: 25 July 2024; AJC-21707

A new ionic copper(II) complex of 1,10-phenanthroline was synthesized and structurally characterized by elemental and spectroscopic analyses, molar conductance and magnetic moment measurements. The crystal structure of complex was also investigated through single crystal X-ray diffraction analysis and suggestted a distorted octahedral geometry around copper(II), where one N atom from 1,10-phenanthroline and three O atoms from three H_2O molecules occupying the basal plane while another N_{phen} and one Cl atom remain at the apical positions. Thus, the presence of three coordinated waters and chloride group along with the counter chloride ion and water of crystallization is responsible for extensive hydrogen bonding present in the molecule. Thus, the complex forms a 3D gigantic H-bonded network. The two types of intermolecular O–H···Cl and O–H···O hydrogen bonding play the pivotal role in crystal packing and plausible conductivity mechanism through the π-π interacting supports. The electrical conductivity and optical properties were also measured and the results focus on the semiconducting nature of the complex with optical band gap (E_{gd}) value 1.23 eV.

Keywords: Complex, Crystal structure, Spectroscopy, Electrical properties, Semiconductor.

INTRODUCTION

Due to several crucial applications in various interdisciplinary scientific worlds, copper(II) complexes of various organic ligands and their derivatives have turn out to be the point of interest of so many researchers. The scientific research shows that the copper(II) complexes have found their profound applications in antibacterial [1], antitumor [2], antimicrobial [3], medicinal [4], catalytic [5], electrochemical [6] and so many other important activities [7-10]. The copper(II) complexes of 1,10-phenanthroline have also been found to show different crystallographic structures and other several applications [11-14]. Moreover, such inorganic metal complexes also draw a remarkable interest in the field of material chemistry [15-18].

The fascinating behaviour of metal complexes with organic ligands is now being accepted as an interdisciplinary area of research by synthetic & material chemists, solid-state physicists, biologists and also by the electrical engineers. The inorganic metal complexes are sometimes being found to behave like semiconducting materials [19,20] and thus this area of research has a stimulating prospect to be explored, especially in the materials and electrical industries. Moreover, sometimes such metal complexes also exhibit many exciting optical properties [21,22] and thus these inorganic metal complexes become a prospective part in applied optoelectronics. Thus, such metal complexes may be used as potential solid-state devices, Schottky diodes [23] and optical sensors [24], which manipulate the semiconducting and optical behaviours of these complexes. As a result of their relevance in the aforementioned contexts, we have been motivated to synthesize and investigate the molecular crystal structure and certain solid-state properties of coordination metal complexes, which have been minimally reported so far.

This is an open access journal, and articles are distributed under the terms of the Attribution 4.0 International (CC BY 4.0) License. This license lets others distribute, remix, tweak, and build upon your work, even commercially, as long as they credit the author for the original creation. You must give appropriate credit, provide a link to the license, and indicate if changes were made.

The aim of this present study is to synthesize and study the crystal structure of a new 1,10-phenanthroline copper(II) complex and explore its semi-conducting nature through the electrical conductivity and optical properties study.

EXPERIMENTAL

1,10-Phenanthroline and cupric chloride were purchased from S.D. Fine Chemicals and Merck, India respectively and used as received. Commercially available spectrograde solvents were used for the physical measurements without further purification. The elemental analyses (carbon, hydrogen and nitrogen) were carried out on Elementar Vario EL III, Carlo Erba 1108 elemental analyzers at the Sophisticated Analytical Instrument Facility (SAIF), Central Drug Research Institute, Lucknow, India. The copper content was estimated by gravimetric method. The electronic spectra were recorded on a Shimadzu UV-2401PC spectrophotometer and infrared spectra (KBr) on a Perkin–Elmer L120-000A spectrophotometer. The molar conductance (10^{-3} M in DMSO/CH_3CN) was measured using a CM-180 Elico conductivity bridge and the magnetic data were measured on a Guoy balance. The UV-vis spectrophotometer (Perkin-Elmer Lambda 2S Double Beam) was employed to study the optical absorption spectra within the wavelength range 300-1100 nm.

Pellets from the synthesized copper(II) complex was prepared with a thickness of 0.1 cm under approximately 1×10^8 Pa pressure for carrying out the conductivity experiment and both the ends of the pellets was painted with silver paste to make the electrical contacts. Then the tablet was placed between two copper electrodes to be tested as ohmic or not. The electrical conductivities of the prepared complex was measured by using two probe methods by measuring the current through the probe with Keithley 6514 high impedance system electrometer, by applying a DC voltage using a Keithley 230 Programmable voltage source. By using the general equation of $\sigma = (I/V_c)(d/a)$, the conductivity was calculated, where I is the current (A), V_c is the potential drop across the sample of cross-sectional area (a) and thickness (d).

Synthesis of copper complex, $[Cu(phen)(H_2O)_3Cl]\cdot Cl\cdot H_2O$: An aqueous solution (30 mL) of $CuCl_2\cdot 2H_2O$ (1.71 g, 10 mmol) was added dropwise to an ethanolic solution (30 mL) of 1,10-phenanthroline (1.81 g, 10 mmol) with constant stirring. The solution mixture was then stirred on water bath for 1 h. The pale blue coloured precipitate was filtered off and the filtrate was kept for slow evaporation. After a week deep blue coloured crystals have been collected. The compound is soluble in DMSO and DMF. Yield: 2.7 g (~70 %). Anal. calcd. (found) % for $C_{12}H_{16}N_2O_4Cl_2Cu$: C, 37.27 (36.88); H, 4.17 (4.06); N, 7.24 (6.99); Cu, 16.43 (15.89). IR (KBr, cm^{-1}): 3350 (ν_{OH}), 1629 ($\nu_{C=N}$, phen), 1547 ($\nu_{C=C}$, phen); UV-vis (DMSO, λ_{max}): 370-380 nm, 555-585 nm and 770-795 nm.

RESULTS AND DISCUSSION

X-ray crystal structure: The X-ray diffraction data of suitable single crystals of the complex was collected on a BRUKER SMART APEX-II CCD X-ray diffractometer furnished with a graphite-monochromated Mo*K*α (λ = 0.71073 Å) radiation, using the ω-scan method at 293 K. The space group determination was done by XPREP and data manipulation (integration and reduction) was performed with SAINT software. The structure was solved by direct method using SHELXS-97 [25] and refined with SHELXL-97 [26] program associated with WINGX system [27] version 1.80.05. The position of Cu ion was determined easily and from the difference Fourier maps O, N and C atoms were consequently determined. All non-hydrogen atoms are anisotropically refined and H atoms are introduced on their carrier atoms and refined with fixed geometry and riding thermal parameters. The crystallographic diagrams were generated using Mercury software [28]. Data related to the X-ray data collection and structure refinement is summarized in Table-1. The crystallographic data has been deposited to the Cambridge Crystallographic Data Centre as supplementary publication material CCDC reference no. 721860. The data can be obtained free of charge *via* http://www.ccdc.cam.ac.uk/conts/retrieving.html (or from the Cambridge Crystallographic Data Centre, 12 Union Road, Cambridge CB2 1EZ, UK; Fax: (+44) 1223-336-033; or Email: deposit@ccdc.cam.ac.uk).

TABLE-1
CRYSTAL DATA AND STRUCTURE
REFINEMENT DETAILS OF THE COMPLEX

Parameters	$[Cu(phen)(H_2O)_3Cl]\cdot Cl\cdot H_2O$
Formula	$C_{12}H_{16}Cl_2CuN_2O_4$
F.W. (g mol^{-1})	386.72
Crystal system	Monoclinic
Space group	*P*2$_1$/n
Crystal colour	Blue
Crystal size (mm^3)	0.28 × 0.22 × 0.18
a (Å)	7.5818(10)
b (Å)	12.3517(16)
c (Å)	16.861(2)
α (°)	90.00
β (°)	102.038(2)
γ (°)	90.00
V $(Å)^3$	1544.3(3)
Z	4
D_c (g cm^{-3})	1.663
μ (mm^{-1})	1.775
F(000)	788.0
T (K)	293
Total reflections	9490
R(int)	0.0266
Unique reflections	3031
Observed reflections	2751
Parameters	222
R_1; wR_2 (I > 2σ(I))	0.0504, 0.1439
GOF (F^2)	1.150
Largest diff peak and hole (e $Å^{-3}$)	0.993, -0.646
CCDC No.	721860

Description of the crystal structure: Slow evaporation of the solvent ethanol-water (1:1) from the filtrate of reaction mixture gave deep blue coloured single crystals appropriate for X-ray structure determination after 1 week. The crystallographic data are summarized in Table-1 and important bond lengths and bond angles are collected in Table-2. The complex crystallizes in monoclinic $P2_1/n$ space group. The molecular

TABLE-2
SELECTED BOND LENGTHS (Å) AND
BOND ANGLES (°) FOR COMPLEX

Distances (Å)			
Cu1-O1	2.051(4)	Cu1-Cl1	2.4303(12)
Cu1-O2	2.055(4)	Cu1-N1	2.071(3)
Cu1-O4	2.065(4)	Cu1 -N2	2.088(4)
Angles (°)			
O1-Cu1-O2	177.66(17)	N1-Cu1-N2	80.43(14)
O1-Cu1-O4	89.92(18)	O1-Cu1-Cl1	91.75(12)
O2-Cu1-O4	89.08(18)	O2-Cu1-N2	88.57(15)
O1-Cu1-N1	90.43(16)	O4-Cu1-N2	92.52(16)
O2-Cu1-N1	90.31(17)	O2-Cu1-Cl1	90.40(11)
O4-Cu1-N1	172.94(15)	O4-Cu1-Cl1	92.33(12)
O1-Cu1-N2	89.37(15)	N1-Cu1-Cl1	94.72(10)
N2-Cu1-Cl1	175.03(11)		

structure of the cationic complex unit $[Cu(phen)(H_2O)_3(Cl)]^+$ of the complex is shown in Fig. 1. The charge on the complex is neutralized by a chloride counter anion present in outer sphere of the complex along with a water of crystallization.

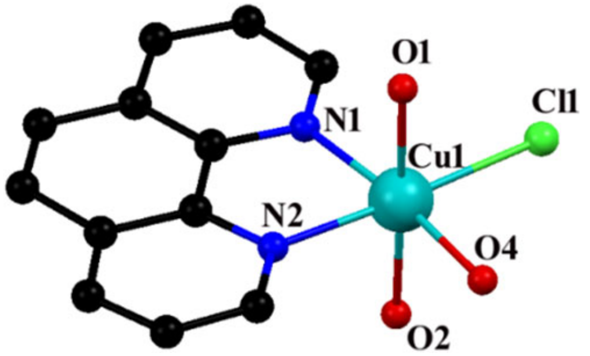

Fig. 1. Molecular structure of the cationic unit of the complex with partial atom numbering scheme. Counter anions and H atoms are omitted for clarity. Colour code: C black, N blue, O red, Cl green and Cu cyan

The Cu(II) ion in the complex remains in octahedral coordination environment of $\{N_2O_3Cl\}$ group of donor atoms. The basal plane of the distorted octahedral geometry around the Cu(II) ion is constructed by three O atoms (O1, O2 and O4) of the water molecule and one phen-N (N1). Along the apical direction there remains one N atom (N2) from phen moiety and the chloride group (Cl1). The Cu–O bond lengths along the basal plane range from 2.051(4) to 2.065(4) Å. The two Cu–N_{phen} distances [Cu1–N1 (basal) = 2.071(3) Å and Cu1–N2 (apical) = 2.088(4) Å] differ significantly due to Jahn-Teller effect commonly encountered for octahedral Cu(II) ions [29]. The tetragonally distorted octahedral complex shows static Jahn–Teller elongation as a consequence of crystal packing (Fig. 2). The *cis*-angles in the octahedron are within the range of 80.43(14)° to 94.72 (10)° and *trans*-angles vary from 172.94(15)° to 177.66(17)°.

The molecule is further stabilized by extensive hydrogen bonding interactions. The two types of intermolecular O–H···Cl and O–H···O hydrogen bonding are operative within the molecule. The coordinated water oxygen O4 is involved in hydrogen bonding with the water (O6) of crystallization whereas each of the other two coordinated waters (O1 and O2) form hydrogen bond with the counter anion (Cl2) and coordinated chlorido group (Cl1*) of other molecule. The coordinated chloride group of one molecular unit is involved in H-bonding interaction with the coordinated water molecules (O1* and O2*) of another molecular unit. Fig. 3 depicts the various types of donor-acceptor interaction present within the complex.

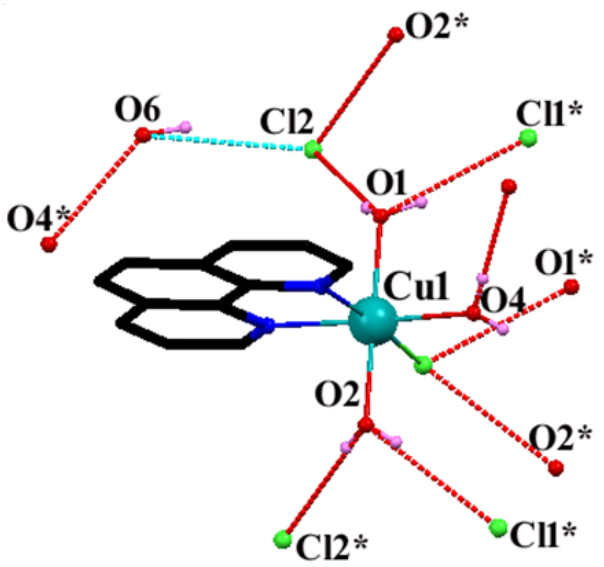

Fig. 3. The H-bonding interaction present within $[Cu(phen)(H_2O)_3Cl]\cdot Cl\cdot H_2O$ complex (*= ½-x, ½+y, ½-z)

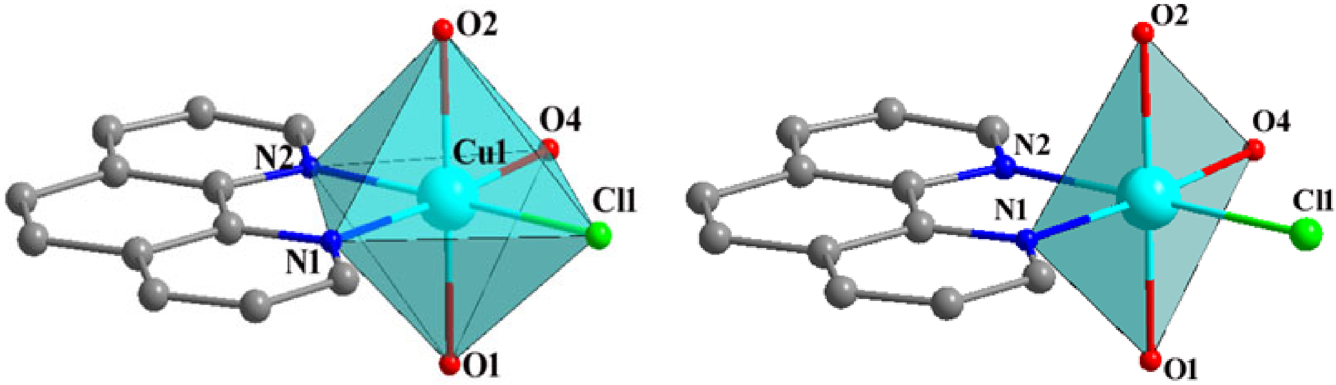

Fig. 2. Core view of the complex showing distorted octahedral geometry around the Cu(II) ion with partial atom numbering scheme [colour code: Cu cyan, N blue, O red, C gray]

The D···A distance varies within the 2.702–3.147 Å range. The presence of extensive H-bonding interaction leads to the formation of a gigantic H-bonded 3D network structure shown in Fig. 4. Due to the extensive intermolecular H-bonding, the phenanthroline groups of the different molecular units come in close proximity which is sufficient enough for the π-π interactions (Fig. 5) to be operative. This π interactions and thus π-π stacking may be the possible reason behind the conductivity of the complex [15,30,31].

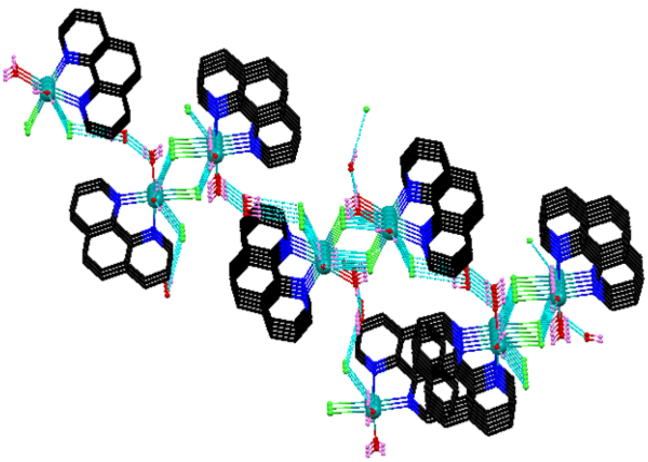

Fig. 4. H-bonded 3D network structure of $[Cu(phen)(H_2O)_3Cl]\cdot Cl\cdot H_2O$ complex

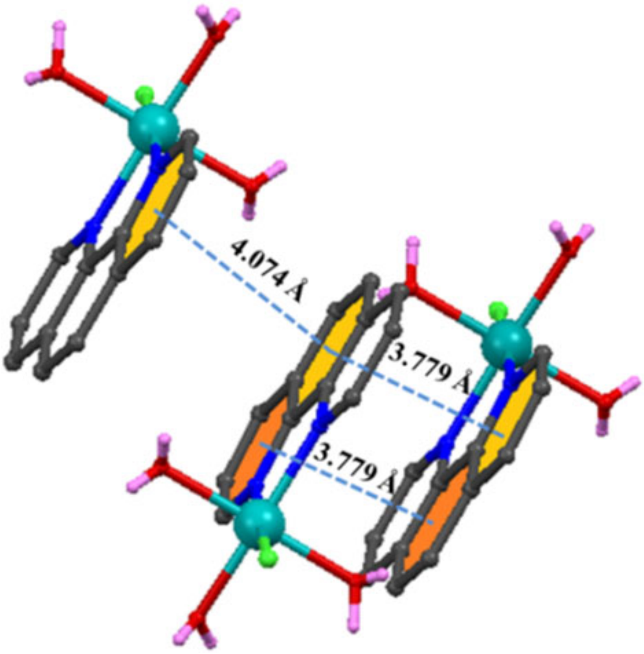

Fig. 5. π-π Interaction operational within the compound

Infrared and electronic spectroscopy: The infrared spectrum of complex, $[Cu(phen)(H_2O)_3Cl]\cdot Cl\cdot H_2O$ shows a broad band centered around 3350 cm^{-1} due to $\nu_{asym}(OH)$ and $\nu_{sym}(OH)$ modes of vibrations of hydrogen bonded non coordinated H_2O molecules. The spectrum also shows two bands at 718 cm^{-1} and 626 cm^{-1} for rocking vibrational mode $\rho_r(H_2O)$ and wagging vibrational mode $\rho_w(H_2O)$, respectively, which indicate the presence of coordinated water molecules within the crystal molecular system [32]. Free 1,10- phenanthroline shows two typical signature bands at 1638 and 1583 cm^{-1} which are assigned for the stretching vibrations of $C{=}N_{(phen)}$ and $C{=}C_{(phen)}$, respectively [33]. But, in copper(II) complex, these bands have been shifted and appeared at 1629 cm^{-1} and 1547 cm^{-1}, respectively. Thus, the shifting towards lower frequencies clearly proves the binding to copper(II) centre through the two pyridyl N atoms of 1,10-phenanthroline [34]. The $\nu_{C\text{-}H(stretching)}$ and $\nu_{C\text{-}H(out\ of\ plane\ bending)}$ are observed at 3048 and 770 cm^{-1}, respectively. A sharp band at 1432 cm^{-1} may be assigned to the bending vibrations of C=C(phen) [35]. Moreover, the ν(Cu-N) and ν(Cu-O) stretching frequencies for the complex appear around *ca.* 450-600 (w/m) cm^{-1} region [34,36], while the ν(Cu-Cl) bands due to Cu–Cl stretches consist of a mixture of medium and intense bands in the complex between 270 and 350 cm^{-1} [37].

It is generally observed that the six-coordinated copper(II) complex with D_{4h} symmetry and ^2D term will first split into E_g and T_{2g} levels and these levels will further spit into B_{1g}, A_{1g}, B_{2g} and E_g levels. So, though, three spin-allowed transitions are expected, in most of the cases two bands are finely resolved [38]. The electronic spectra of the present copper(II) complex (Fig. 6) shows three absorption spectral bands, where the broad bands in the region at 555-585 nm and 770-795 nm may be assigned to $^2B_{1g}\rightarrow{}^2B_{2g}$ and $^2B_{1g}\rightarrow{}^2A_{1g}$ transitions, which suggest a distorted octahedral geometry of the copper(II) complex [39,40] due to Jahn-Teller distortion. The appearance of broad band around 370-380 nm may be attributed to π-π* transition of the 1,10-phenanthroline system [41].

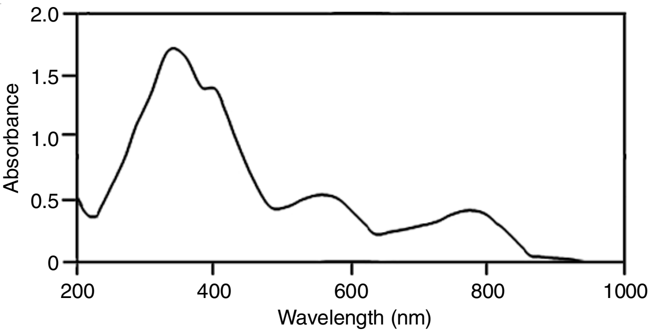

Fig. 6. Electronic spectrum of $[Cu(phen)(H_2O)_3Cl]\cdot Cl\cdot H_2O$ complex

Magnetic moments and molar conductance: The effective magnetic moment (μ_{eff}) value for complex was found to be 1.86 B.M., which fairly corresponds to the presence of one unpaired electrons (S = 1) with configuration ($t_{2g}^6e_g^3$) of copper(II) in almost octahedral environment [42]. It further indicates the absence of any spin-spin coupling between the unpaired electrons of two intermolecular Cu(II) systems. The slight increase from the spin-only value *i.e.* 1.73 B.M. may be attributed due to spin-orbit coupling or orbital contribution of the unpaired electron in its ground state [43].

The molar conductance data of the complex shows the different values with changing the solvent system. In DMSO and CH_3CN, the molar conductance of the complex are found to be 89 and 116 Ω^{-1} cm^2 mol^{-1} indicating the 1:1 electrolytic nature of the complex. The variation may be attributed to the difference in polarity and density of the solvents. The higher molar conductance in CH_3CN compared to DMSO may be due to the higher polarity and lower density of CH_3CN [44].

Electrical conductivity: The variation of electrical conductivity (logarithmic values) with reciprocal of absolute temperature for the copper complex was measured and presented in Fig. 7. The conductivity of the complex was measured at the range of 300-500 K and a typical temperature dependence of the electrical conductivity was observed during heat treatment. The temperature dependence of the electrical conductivity of any semiconducting material is expressed by the following Arrhenius equation [45]:

$$\sigma = \sigma_0 \exp\left(-\frac{\Delta E_a}{kT}\right)$$

where σ_0 is the pre-exponential factor and it depends on the semiconducting nature of material, ΔE_a is the thermal activation energy for electron transfer process and k is the Boltzmann constant. The slope of the straight line obtained from the plot of ln σ *versus* 1000/T, has been utilized to determine the thermal activation energies of the complex.

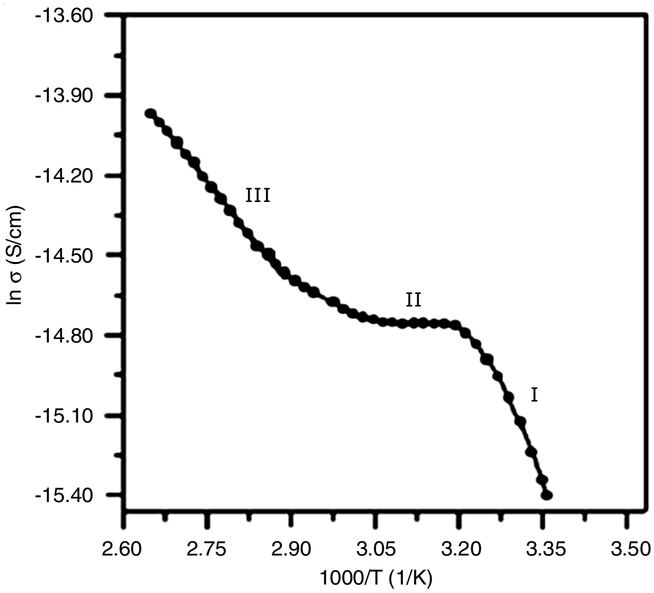

Fig. 7. Temperature of electrical conductivity of $[Cu(phen)(H_2O)_3Cl]\cdot Cl\cdot H_2O$ complex

The temperature dependence of the electrical conductivity curve shows that the curve possesses three distinct regions I, II and III. The positive temperature coefficient of electrical conductivity has been observed in case of regions I and III, whereas, the region II shows a negative value. It indicates that the activation energies of electrical conductivity of the complex have positive value in regions I and III, but negative values in region II. The extrinsic behaviour is observed in region I, that is, in this region the conductivity is increased exponentially with increase in temperature. The activation from the donor level to the conduction band is responsible for such extrinsic behaviour and the activation energy is determined at the donor energy level [45].

A slight decrease of conductivity with temperature is observed in region II, which may be due to the scattering of carriers by photons. Moreover, such scattering actually arises owing to lattice vibrations within the temperature range and the magnitude depends on the crystal structure of the complex [46,47]. Further, a positive temperature coefficient of electrical conductivity is observed in region III, but the activation energy is found to have lower value than that of region I. So, it may designate the region III as the intrinsic region of conductivity, which indicates that the activation takes place from the valence band to the conduction band. So, the calculated activation energies correspond to different higher and lower energy levels. The high activation energy values are possibly associated with the electronic transitions between the valence bands or the localized levels at the bottom of the conduction bands. However, thermally activated electron hopping process may be responsible for the low activation energies of the complex. Thus, in general, these two kinds of activation energies are thought to be associated with the conductivity process either through intramolecular or intermolecular fashion. Particularly, the intramolecular conduction process is responsible for the higher values of ΔE_a, while the lower values of ΔE_a are linked to the intermolecular conduction process.

In complexes having semiconducting properties, the conductivity arises due to transfer of carrier body within the complex by two ways, one is intramolecular and another is intermolecular movement of the current carrier. When orbitals with almost same energy levels are available, the hopping of electrons from one atomic site to another is observed during the intramolecular transfer. This intramolecular electronic transport generally occurs between the metal and ligand orbitals. But, when the intermolecular overlap between the orbitals of same energy level takes place, the thermally activated movements of either electrons or holes are occurred from one molecular system to another one. The movement of π-electrons within the molecular complexes of comparable energy states is also acceptable. Between the two, inter- and intramolecular conduction processes, the former with lower activation energy is assumed to be the initial step of the conduction process, though, both the inter- and intramolecular transfers are considered for considering the total conductivity of the complex.

The complex exhibits extrinsic behavior between 300 and 315 K, a small decrease in conductivity between 320 and 335 K (possibly caused by photon scattering) and then a sharp increase in intrinsic behaviour between 335 and 380 K, as shown in the Arrhenius plot of ln σ *vs.* 1000/T. The conductivity remains almost constant between 315-320 K and may be compared with exhausting region. So, the curve purely resembles to that of a semiconductor. The slope in the extrinsic region for an n-type semiconductor is given by $(E_g - E_d)/k$ and $E_g/2k$ in the intrinsic region. The activation energies (E_a) for the extrinsic and intrinsic regions are given in Table-3. Thus, the conductivity of copper complex typically shows an n-type semiconducting behaviour which means that most of the carriers involved in the transport process are negatively charged electrons.

Two plausible mechanistic pathways may be proposed to explain the n-type semiconductivity in the metal complex [15]. In the first model, it is assumed that the electron hops from one localized metal site to another one. After reaching the new

TABLE-3
ELECTRONIC PARAMETERS OF COMPLEX

Complex	E_a(I) (eV)	E_a(II) (eV)	E_{gd} (eV)
$[Cu(phen)(H_2O)_3Cl]\cdot Cl\cdot H_2O$	1.34	0.79	1.23

E_a: activation energy of electrical conduction; E_{gd}: energy gap for directly allowed transitions.

metal site, it compels the surrounding molecular systems to adjust their localization and thus the electron gets trapped temporarily in the potential well and resides until it gets thermally activated further for migrating to another neighboring metal site. Thus the electrons are supposed to tunnel from one molecular site to another adjacent equivalent molecular site. In such tunneling of electrons [48], the intermolecular H-bonding and π-π interactions [15,30,31] are supposed to promote the electrons to cross the intermolecular potential barriers. In this case, the holes have the minimum role on the movement of negative charge. On the other hand, the second way of conduction process may involve the excitation of electrons from the HOMO to LUMO of π-MOs through delocalization of the π-cloud and such movements of π-electrons help to switch over the metal complex to its semiconducting state.

Optical properties: The variation of optical absorption with the corresponding wavelength is shown in Figs. 8 and 9. The optical spectra were recorded at room temperature and the fundamental absorption edge is analyzed with the theory of Mott & Davis [49]. From the recorded optical spectra, the energy band gaps and the nature of the optical transition, *i.e.* both allowed and forbidden, involved in the complex, can easily be obtained.

The optical data have been analyzed and the optical band gaps of the complex were determined using the following classical relation for near edge optical absorption in semiconductors [50]:

$$\alpha h\nu = A(h\nu - E_g)^n \qquad \text{(i)}$$

where α is the linear absorption coefficient, ν is the frequency, h is Planck's constant, E_g is the energy gap between the top of the valence band and bottom of conduction band at the same value of wavenumber (k) and n depends on the kind of prevailing optical transitions. Specifically, n is 1/2, 3/2 for transitions which are directly allowed and directly forbidden, whereas, for indirectly allowed and indirectly forbidden transitions n is 2 and 3, respectively, A is a constant involving the properties of the bands. Thus, the energy gap for directly allowed (E_{gd}) and indirectly allowed (E_{gi}) transitions can be calculated using the following relations:

$$\alpha h\nu = A_a(h\nu - E_{gd})^{1/2} \qquad \text{(ii)}$$

and

$$\alpha h\nu = A_i(h\nu - E_{gi})^2 \qquad \text{(iii)}$$

where, A_a and A_i are the characteristic parameters for the respective direct and indirect transitions, independent of ν. From eqns. ii and iii, the linear extrapolation towards zero absorption will correspond to direct (E_{gd-}) and indirect (E_{gi}) band gaps respectively. The values of the optical band gap E_{gd} was determined from Figs. 8 and 9 by the least squares fitting of the data and the obtained values were given in Table-3.

Conclusion

The synthesis, characterization and molecular structure of a new copper(II) complex with 1,10-phenanthroline ligand has been reported. The single crystal X-ray analysis shows that the new copper(II) complex, $[Cu(phen)(H_2O)_3Cl]\cdot Cl\cdot H_2O$, possesses a distorted octahedral geometry which is getting stabilized through the intermolecular O–H···Cl and O–H···O hydrogen bonding interactions. It was further observed from the results of electrical conductivity and optical properties that the complex shows typical n-type semiconducting properties and a direct band gap. The conduction mechanism is operated by electron hopping and through π-π interactions. So, the complex may be utilized as potential applied material.

ACKNOWLEDGEMENTS

One of the authors (S.S.) is thankful to the authorities of Chakdaha College for providing the laboratory facilities. SS is also thankful to Prof. A.P. Chattopadhyay, Ex-Professor in Chemistry, University of Kalyani for some useful spectroscopic discussions.

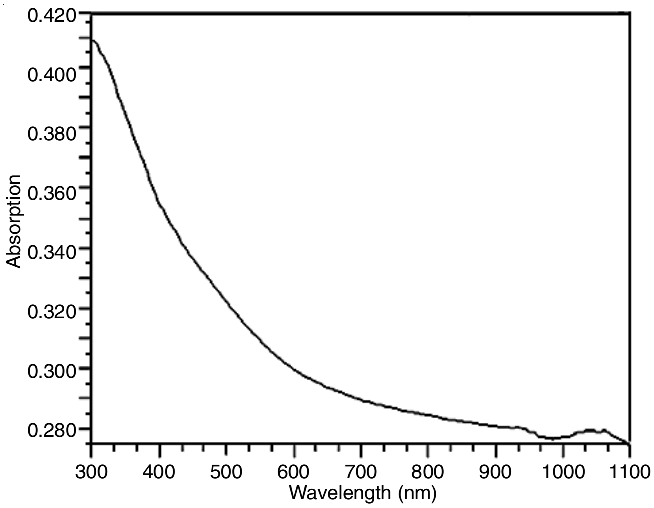

Fig. 8. Optical absorption spectrum of $[Cu(phen)(H_2O)_3Cl]\cdot Cl\cdot H_2O$ complex

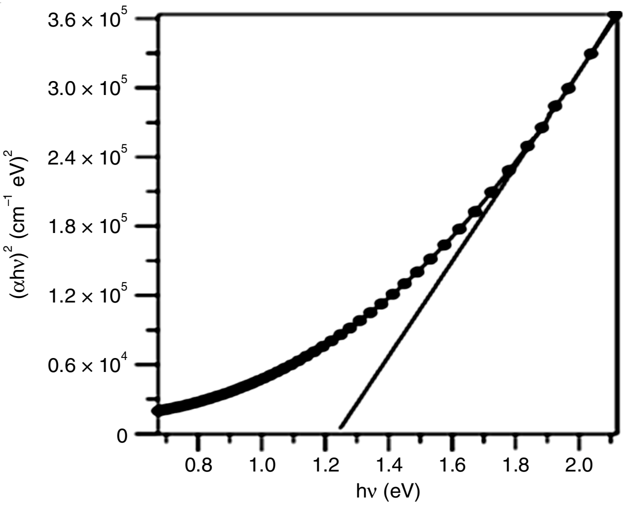

Fig. 9. Plot of $(\alpha h\nu)^2$ *vs.* hν of $[Cu(phen)(H_2O)_3Cl]\cdot Cl\cdot H_2O$ complex

CONFLICT OF INTEREST

The authors declare that there is no conflict of interests regarding the publication of this article.

REFERENCES

1. S. Rajalakshmi, A. Fathima, J.R. Rao and B.U. Nair, *RSC Adv.*, **4**, 32004 (2014); https://doi.org/10.1039/C4RA03241A
2. V.C. da Silveira, J.S. Luz, C.C. Oliveira, I. Graziani, M.R. Ciriolo and A.M.C. Ferreira, *J. Inorg. Biochem.*, **102**, 1090 (2008); https://doi.org/10.1016/j.jinorgbio.2007.12.033
3. D.C. Ilies, E. Pahontu, S. Shova, R. Georgescu, N. Stanica, R. Olar, A. Gulea and T. Rosu, *Polyhedron*, **81**, 123 (2014); https://doi.org/10.1016/j.poly.2014.05.074
4. X.Y. Qin, Y.N. Wang, X.P. Yang, J.J. Liang, J.L. Liu and Z.H. Luo, *Dalton Trans.*, **46**, 16446 (2017); https://doi.org/10.1039/C7DT03242K
5. A. Bhattacharjee, S. Halder, K. Ghosh, C. Rizzoli and P. Roy, *New J. Chem.*, **41**, 5696 (2017); https://doi.org/10.1039/C7NJ00846E
6. J. Losada, I. Del Peso and L. Beyer, *Inorg. Chim. Acta*, **321**, 107 (2001); https://doi.org/10.1016/S0020-1693(01)00511-4
7. S.M. Leite, L.M. Lima, S. Gama, F. Mendes, M. Orio, I. Bento, A. Paulo, R. Delgado and O. Iranzo, *Inorg. Chem.*, **55**, 11801 (2016); https://doi.org/10.1021/acs.inorgchem.6b01884
8. F. Ouyang, X. Jiang, X. Liu, Y. Chen, Y. Chen, S. Chen and L. Jia, *Transition Met. Chem.*, **46**, 315 (2021); https://doi.org/10.1007/s11243-021-00448-6
9. X.H. Bu, M. Du, Z.L. Shang, R.H. Zhang, D.Z. Liao, M. Shionoya and T. Clifford, *Inorg. Chem.*, **39**, 4190 (2000); https://doi.org/10.1021/ic000094d
10. L. Rigamonti, F. Demartin, A. Forni, S. Righetto and A. Pasini, *Inorg. Chem.*, **45**, 10976 (2006); https://doi.org/10.1021/ic0613513
11. S. Masuri, E. Cadoni, M.G. Cabiddu, F. Isaia, M.G. Demuru, L. Morán, D. Bucek, P. Vanhara, J. Havel and T.P. Lukáš, *Metallomics*, **12**, 891 (2020); https://doi.org/10.1039/d0mt00006j
12. L. Polloni, A.C. Seni Silva, S.C. Teixeira, F.V.P.V. Azevedo, M.A.P. Zóia, M.S. da Silva, P.M.A.P. Lima, L.I.V. Correia, J. do Couto Almeida, C.V. da Silva, V.M. Rodrigues Ávila, L.R.F. Goulart, S. Morelli, W. Guerra and R.J. Oliveira Júnior, *Biomed. Pharmacother.*, **112**, 108586 (2019); https://doi.org/10.1016/j.biopha.2019.01.047
13. Y.Y. Wang, X. Wang, Q.Z. Shi and Y.C. Gao, *Transition Met. Chem.*, **27**, 481 (2002); https://doi.org/10.1023/A:1015617327024
14. O.O. Onawumi, F.A. Adekunle, A.O. Ibrahim, M.V. Rajasekharan and O.A. Odunola, *Synth. React. Inorg. Met.-Org. Nano-Met. Chem.*, **40**, 78 (2010); https://doi.org/10.3109/10799890903555673
15. S. Sarkar, S. Biswas, M.S. Liao, T. Kar, Y. Aydogdu, F. Dagdelen, G. Mostafa, A.P. Chattopadhyay, G.P. Yap, R.H. Xie, A.T. Khan and K. Dey, *Polyhedron*, **27**, 3359 (2008); https://doi.org/10.1016/j.poly.2008.07.034
16. S. Sarkar, Y. Aydogdu, F. Dagdelen, B.B. Bhaumik and K. Dey, *Mater. Chem. Phys.*, **88**, 357 (2004); https://doi.org/10.1016/j.matchemphys.2004.08.001
17. Y. Aydogdu, F. Yakuphanoglu, A. Aydogdu, M. Sekerci, Y. Balci and I. Aksoy, *Synth. Met.*, **107**, 191 (1999); https://doi.org/10.1016/S0379-6779(99)00167-8
18. A. Dutta, A. Mahanta, S.J. Panda, S. Biswas, V.B. Kamble, C.S. Purohit, S.K. Jasimuddin and R. Ghosh, *J. Chem. Sci.*, **135**, 62 (2023); https://doi.org/10.1007/s12039-023-02179-w
19. Y. Aydogdu, F. Yakuphanoglu, F. Dagdelen, M. Sekerci and I. Aksoy, *Mater. Lett.*, **57**, 237 (2002); https://doi.org/10.1016/S0167-577X(02)00772-3
20. S. Biswas, F. Dagdelen, Y. Aydogdu and K. Dey, *Mater. Chem. Phys.*, **129**, 1121 (2011); https://doi.org/10.1016/j.matchemphys.2011.05.071
21. K. Kalyanasundaram and M. Grätzel, *Coord. Chem. Rev.*, **177**, 347 (1998); https://doi.org/10.1016/S0010-8545(98)00189-1
22. W.C. Choy, W.K. Chan and Y. Yuan, *Adv. Mater.*, **26**, 5368 (2014); https://doi.org/10.1002/adma.201306133
23. K. Akkiliç, Y.S. Ocak, T. Kiliçoglu, S. Ilhan and H. Temel, *Curr. Appl. Phys.*, **10**, 337 (2010); https://doi.org/10.1016/j.cap.2009.06.019
24. W.W. Lee, K.Y. Wong and X.M. Li, *Anal. Chem.*, **65**, 255 (1993); https://doi.org/10.1021/ac00051a012
25. G.M. Sheldrick, SHELXS-97 and SHELXL-97, Program for Crystal Structure Solution and Refinement, University of Gottingen, Gottingen (1997).
26. G.M. Sheldrick, *Acta Crystallogr. A*, **64**, 112 (2008); https://doi.org/10.1107/S0108767307043930
27. L.J. Farrugia, *J. Appl. Cryst.*, **32**, 837 (1999); https://doi.org/10.1107/S0021889899006020
28. C.F. Macrae, I.J. Bruno, J.A. Chisholm, P.R. Edgington, P. McCabe, E. Pidcock, L. Rodriguez-Monge, R. Taylor, J. van de Streek and P.A. Wood, *J. Appl. Cryst.*, **41**, 466 (2008); https://doi.org/10.1107/S0021889807067908
29. K. Chattopadhyay, B.K. Shaw, S.K. Saha and D. Ray, *Dalton Trans.*, **45**, 6928 (2016); https://doi.org/10.1039/C6DT00103C
30. X. Chen, F. Gao and W. Yang, *Sci. Rep.*, **6**, 29314 (2016); https://doi.org/10.1038/srep29314
31. X. Chen, B. Ma, X. Wang, S. Yao, L. Ni, Z. Zhou, Y. Li, W. Huang, J. Ma, J. Zuo and X. Wang, *Chem. Eur. J.*, **18**, 11828 (2012); https://doi.org/10.1002/chem.201103972
32. R. Banik, S. Roy, A. Bauza, A. Frontera and S. Das, *RSC Adv.*, **5**, 10826 (2015); https://doi.org/10.1039/C4RA10251G
33. X. Wang, G. Jia, Y. Yu, Y. Gao, W. Zhang, H. Wang, Z. Cao and J. Liu, *Quim. Nova*, **38**, 298 (2015).
34. O.A. Dar, S.A. Lone, M.A. Malik, M.Y. Wani, A. Ahmad and A. Hashmi, *RSC Adv.*, **9**, 15151 (2019); https://doi.org/10.1039/C9RA02600B
35. A. Abebe and T. Hailemariam, *Bioinorg. Chem. Appl.*, **2016**, 3607924 (2016); https://doi.org/10.1155/2016/3607924
36. H.-Y. Mao, X.-Q. Shen, G. Li, H.-Y. Zhang, C. Xu, H.-L. Liu, E.-B. Wang, Q.-A. Wu, H.-W. Hou and Y. Zhu, *Polyhedron*, **23**, 1961 (2004); https://doi.org/10.1016/j.poly.2004.04.034
37. M. Goldstein, E.F. Mooney, A. Anderson and H.A. Gebbie, *Spectrochim. Acta*, **21**, 105 (1965); https://doi.org/10.1016/0371-1951(65)80109-6
38. S. Chandra and S.D. Sharma, *Transition Met. Chem.*, **27**, 732 (2002); https://doi.org/10.1023/A:1020309322470
39. P.M. Reddy, R. Rohini, E.R. Krishna, A. Hu and V. Ravinder, *Int. J. Mol. Sci.*, **13**, 4982 (2012); https://doi.org/10.3390/ijms13044982
40. S. Chandra and L.K. Gupta, *Spectrochim. Acta A Mol. Biomol. Spectrosc.*, **60**, 1563 (2004); https://doi.org/10.1016/j.saa.2003.08.023
41. Y. Li, N. Dandu, R. Liu, Z. Li, S. Kilina and W. Sun, *J. Phys. Chem. C*, **118**, 6372 (2014); https://doi.org/10.1021/jp411259f
42. J. Lewis and R.A. Walton, *J. Chem. Soc. A*, 1559 (1966); https://doi.org/10.1039/j19660001559
43. B.N. Figgis and J. Lewis, in eds.: J. Lewis and R. G. Wilkins, The Magnetochemistry of Chelates, In: Modern Coordination Chemistry. Interscience, New York, USA (1960).
44. I. Ali, W.A. Wani and K. Saleem, *Synth. React. Inorg. Met.-Org. Nano-Met. Chem.*, **43**, 1162 (2013); https://doi.org/10.1080/15533174.2012.756898
45. F. Gutmann and L.E. Lyons, Organic Semiconductors, Wiley Interscience, New York (1967).
46. M.S. Masoud, E.A. Khalil and M.E. Kassem, *React. Solids*, **2**, 269 (1986); https://doi.org/10.1016/0168-7336(86)80090-0
47. M.S. Masoud, S.A. El-Enein and E. El-Shereafy, *J. Therm. Anal.*, **37**, 365 (1991); https://doi.org/10.1007/BF02055938
48. Y. Aydogdu, F. Yakuphanoglu, A. Aydogdu, S. Saydam, M. Sekerci and F.S. Boydag, *Synth. Met.*, **122**, 329 (2001); https://doi.org/10.1016/S0379-6779(00)00360-X
49. N.F. Mott and E.A. Davis, Electronic Processes in Non-crystalline Materials. Clarendon Press, Oxford, New York (1971).
50. J.I. Pankove, Optical Processes in Semiconductors. Prentice-Hall Inc., New Jersey (1971).